JOURNAL OF MATERIALS SCIENCE 25 (1990) 2520–2526

Glass dispersion favours ionic conduction in $6Li_2SO_4$–$4Li_2CO_3$ composite solid electrolyte

K. SINGH, S. S. BHOGA
Department of Physics, Nagpur University Campus, Nagpur 440 010, India

The effect of a dispersion of $7Li_2O$–$3B_2O_3$ glass on the electrical conductivity of $6Li_2SO_4$–$4Li_2CO_3$ eutectic has been studied. The samples were prepared by two different methods. With the dispersion of glass into the crystalline matrix a prominent increase in the conductivity has been observed. The results have been explained in the light of dispersed phase theory using microstructural evidence. These results would provide a new approach for achieving an enhancement in the ionic conductivity of solid electrolytes.

1. Introduction

In electrochemical devices, polycrystalline ionic conductors rather than single crystals are used due to the ease of their fabrication in required shapes and isotropy in their electrical and mechanical properties [1].

The phase diagram study of the Li_2SO_4–Li_2CO_3 system reveals the presence of a eutectic composition at 60 : 40 mol % ratio [2]. It has been reported by Deshpande and Singh [3] that the eutectic composition gives maximum conductivity in the entire series. The enhancement in the conductivity of the eutectic has been observed by addition of LiX (X = F, Cl, Br and I) and Na_2SO_4 [4].

Several attempts have been made in the past to enhance the conductivity of lithium ion conducting solid electrolytes. In this direction essentially the following approaches have been adopted: (i) optimization of preparative parameters [5], (ii) the aliovalent substitution of the conducting cation [6, 7], (iii) trapping of high-temperature highly conducting phases at room temperature [8], (iv) stabilization of open channel structure [9], (v) increasing the disorder of the system (e.g. Li^+ conducting glasses [10]), and (vi) dissolution of ionic salts in polymers and glasses [11–13].

The dispersion of a second phase into an otherwise poor ionic conductor has become a new strategy in materials research for conductivity enhancement [14]. Liang [15] was the pioneer in this field, and observed a remarkable enhancement of ionic conductivity in LiI–Al_2O_3. The work on composite solid electrolytes has been reviewed in a recent article by Poulsen [16]. It is evident from the literature that the dispersion of conducting glass particles in a crystalline matrix has remained untouched so far. This has stimulated interest in investigating the effect of Li_2O–B_2O_3 glass dispersion on the electrical conductivity of $6Li_2SO_4$–$4Li_2CO_3$ eutectic.

2. Experimental procedure

The initial ingredients Li_2SO_4, Li_2CO_3, Li_2O and B_2O_3 with purity greater than 99% were procured from Fluka AG, Germany. Well-dried 60 mol % Li_2SO_4 and 40 mol % Li_2CO_3 were mixed thoroughly under acetone and heated in a platinum crucible. The temperature of the furnace was maintained 300 K above the melting point for homogenization of the melt. The melt was then quenched in an aluminium mould at room temperature. The glass Li_2O–B_2O_3 (70 : 30) used (selected on the basis of high Li^+ conductivity) as a dispersoid in the present study was prepared by the copper-drum quenching technique. The eutectic and glass were crushed separately and sieved to get a fine powder of average particle size $< 45\ \mu m$. The eutectic with 10, 20 and 30 wt % of glass was mixed thoroughly under acetone. Thereafter, the samples were prepared by two different methods:

Method I. A weighed amount of mixture was pressed at 10 ton cm^{-2} to get a pellet of dimensions 12 mm diameter and 0.5 mm thickness. These pellets were sintered at 673 K for an hour followed by quenching at room temperature.

Method II. In this case the mixture was heated in a platinum crucible above the melting point for an hour to homogenize the melt, and then rapidly quenched in an aluminium mould at room temperature. The samples were ground to prepare rectangular specimens having dimensions 7 mm × 5 mm × 3 mm.

The prepared samples were characterized by X-ray diffraction (XRD) and differential thermal analysis (DTA) with the help of a Philips X-ray diffractometer PW 1700 using Cu$K\alpha$ radiation and a Perkin-Elmer thermal analyser respectively. The microstructures were observed using a Cambridge 250 mark III scanning electron microscope (SEM). For electrical conductivity measurements, ohmic contacts were ensured by using aluminium foils and spring-loading the specimen between the two silver electrodes of the sample holder as described elsewhere [17]. Before measurement, the sample was heated in an electric furnace at 633 K for 2 h to remove the moisture therein. The a.c. electrical conductivity was measured as a function of frequency from 10 Hz to 13 MHz at various temperatures in the range 633 to 423 K during the cooling

0022–2461/90 $03.00 + .12 © *1990 Chapman and Hall Ltd.*

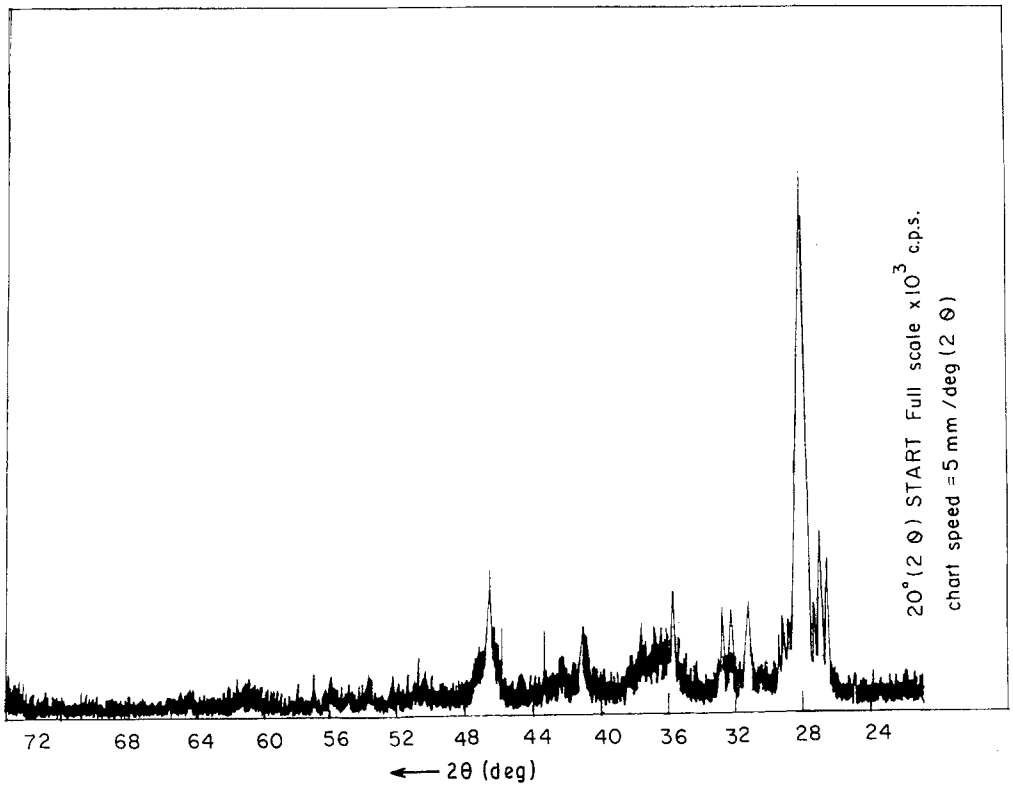

Figure 1 XRD pattern of 20 wt % glass-dispersed $6Li_2SO_4$–$4Li_2CO_3$ eutectic.

cycle, at intervals of 20° C, using an HP 4192 A LF impedance analyser. The temperature was controlled to ± 1° C with the help of a Eurotherm (UK) temperature controller.

The d.c. polarization method based on the perfectly ion-blocking effect of silver electrodes was used to determine the partial electronic conductivity with the help of a Keithley 617 programmable electrometer.

3. Results and discussion

The room-temperature XRD pattern for 20 wt % glass-dispersed composite is shown in Fig. 1. The values of d and I/I_0 obtained from the figure are tabulated in Table I. It can be noted that the experimentally observed values of d are in good agreement with those of ASTM data for Li_2SO_4, $Li_2SO_4 \cdot H_2O$ and Li_2CO_3 phases. Also, no peaks corresponding to crystalline Li_2O, B_2O_3 and LiOH or intermediate new phases are observed. Thus it can be concluded that the unreacted glass is dispersed into the Li_2SO_4–Li_2CO_3 eutectic. The transference number measurements (Fig. 2) show that the contribution of the electronic component (σ_e) to the total conductivity ($\sigma_T = \sigma_i + \sigma_e$) is less than 0.004% in the temperature range from 300 to 623 K, which is negligibly small.

TABLE I Comparison of the experimentally obtained d and I/I_0 values with ASTM data for 20 wt % glass-dispersed $6Li_2SO_4$–Li_2CO_3 eutectic prepared by Method I

Observed		ASTM		Observed phase (hkl)	
d (nm)	I/I_0	d (nm)	I/I_0		
0.50851	30	0.5084	100	$Li_2SO_4 \cdot H_2O$	$(\bar{1}\,0\,1)$
0.41605	34	0.416	85	Li_2CO_3	(1 1 0)
0.39973	100	0.400	100	Li_2SO_4	$(\bar{1}\,1\,1)$
0.39198		0.392	40	Li_2SO_4	(2 0 0)
0.38367	18.6	0.3837	85	$Li_2SO_4 \cdot H_2O$	(1 0 1)
0.35567	33	0.3559	90	$Li_2SO_4 \cdot H_2O$	(1 1 0)
0.31602	29	0.316	40	Li_2SO_4	(2 0 1)
0.30462	20	0.3046	20	Li_2CO_3	(1 1 1)
0.30294	13	0.303	25	Li_2CO_3	(1 1 1)
0.29455	24	0.2944	50	$Li_2SO_4 \cdot H_2O$	(1 1 2)
0.28175	15	0.2812	100	Li_2CO_3	(0 0 2)
0.27937	15	0.2792	10	Li_2SO_4	$(\bar{2}\,1\,2)$
0.26638	9	0.2665	4	Li_2SO_4	(2 1 1)
0.26285	9	0.2628	8	Li_2SO_4	(2 0 3)
0.24830	15	0.2479	20	Li_2SO_4	(0 2 0)
0.24368	20	0.2405	35	$Li_2SO_4 \cdot H_2O$	(0 2 0)
0.15992	5	0.1595	8	Li_2CO_3	$(\bar{4}\,2\,1)$

The total conductivity of each sample (excluding electrode effects) was determined from the real-axis intercept of the complex impedance plot. Plots of $\log \sigma T$ against $10^3/T$ for various composites prepared by Method I are displayed in Fig. 3. From this figure it can be seen that, in general, the conductivity increases by four orders of magnitude with increase in temperature from 423 to 573 K. This enhancement can be attributed to the thermally activated cationic conductivity. It is also evident that the conductivity of the dispersed solid electrolyte system (DSES composite) increases with the concentration of glass. It exhibits a maximum at 20 wt % of glass and starts decreasing thereafter. The variation of activation energy with glass content is opposite to that of conductivity. These results are similar to those for LKCN–γ-Al_2O_3 composites reported by Liquan [18]. It is also interesting to note that after sintering of the pellet at 673 K (for an hour) the conductivity decreases.

Figs 4a to d display microphotographs of unsintered and sintered pellets before glass dispersion, and with dispersion of 10 and 20 wt % glass, for $6Li_2SO_4$–$4Li_2CO_3$ eutectic samples prepared by Method I. Figs 4a and b reveal that, after sintering the eutectic sample, grain growth takes place at the cost of pores

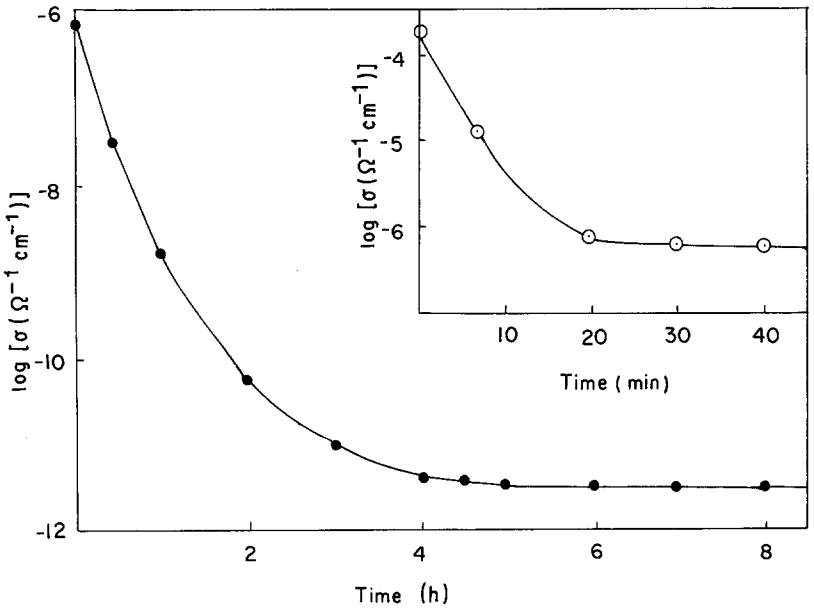

Figure 2 Variation of d.c. conductivity with time for transport number determination at (●) 300 and (⊙) 623 K.

resulting in a reduction of the interfacial area between the grains. However, this sintering time and temperature are inadequate to make the sample totally free of voids. According to Dissanayake and Mellander [2], the maximum conductivity in a two-phase (ionic conducting) mixture is associated with minimum grain size, giving rise to a maximum (highly conducting) interfacial area between the grains. This explains the reduction in the ionic conductivity due to sintering. On the other hand, when 10 wt % of glass is added to the eutectic, pelletized and then sintered at 673 K (by Method I, well above T_g = 568 K), the glass may be in a semi-molten state and flow across the grain boundaries to fill the voids. Further, on quenching the pellet, this glass gets solidified into nearly spherical-shaped isolated particulates as depicted in Fig. 4c. Furthermore, from Fig. 4d it is clearly seen that, with increase in concentration of glass, it covers the crystalline grains and grows in irregular shape. This in turn gives rise to voids in the composite sample, and hence to a decrease in conductivity.

The Arrhenius plots for composites prepared by Method II are depicted in Fig. 5. It is evident from this figure that the conductivity of the glass is higher than that of the $6Li_2SO_4$–$4Li_2CO_3$ eutectic throughout the temperature range of investigation. The ionic conductivity of the eutectic increases with the concentration of glass up to 20 wt %. Samples with glass content > 20 wt % were difficult to quench (at room temperature) due to their high viscosity. SEM photographs for the samples with 10 and 20 wt % glass along with the host system (eutectic) are shown in Figs. 6a to c. These

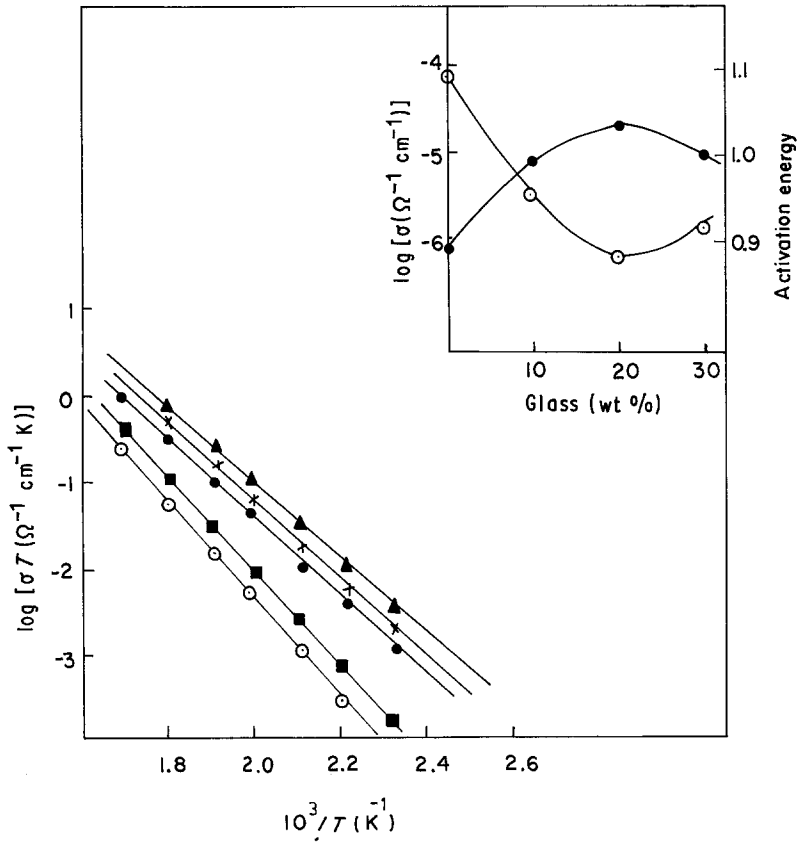

Figure 3 Variation of log σT with $10^3/T$ for samples prepared by Method I: (■) unsintered eutectic, (⊙) sintered eutectic, (●) eutectic + 10 wt % glass, (▲) eutectic + 20 wt % glass, (×) eutectic + 30 wt % glass. Inset: (●) log σ and (⊙) activation energy against wt % glass.

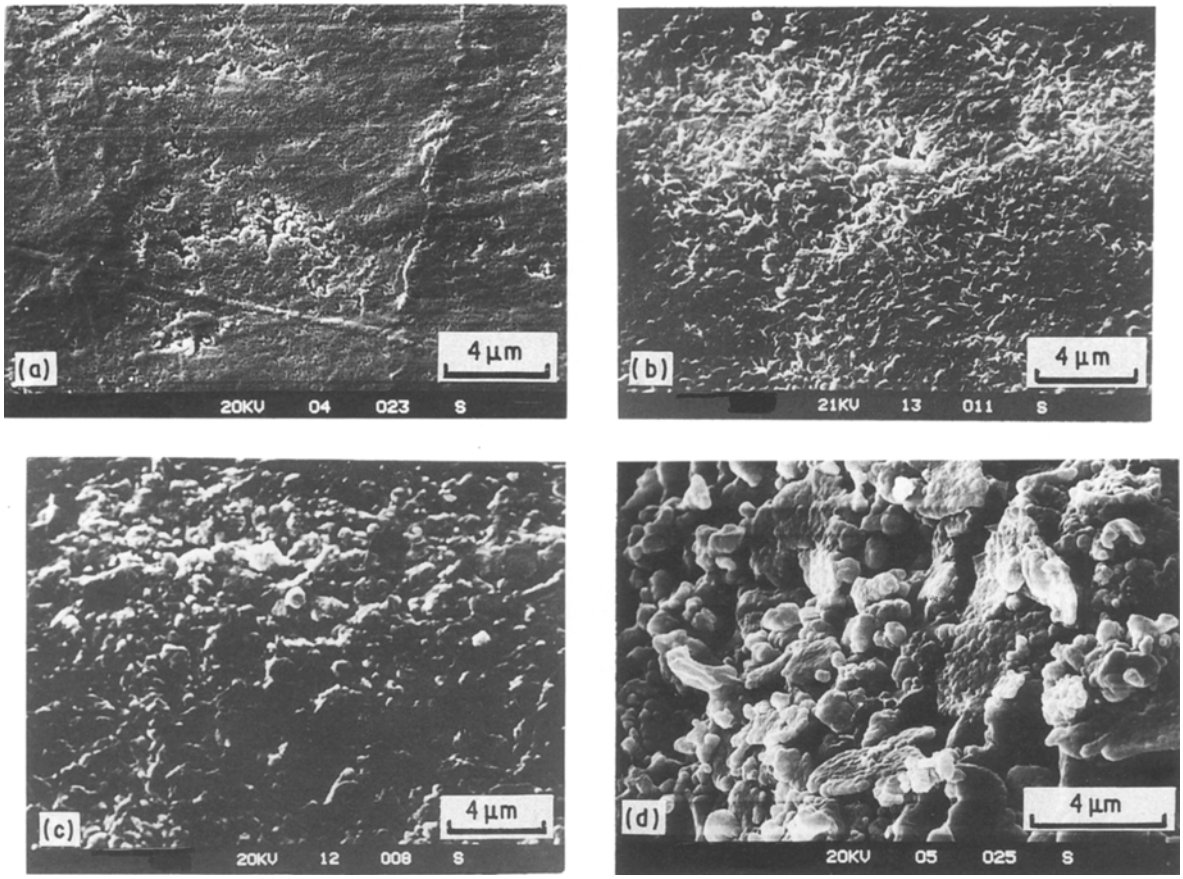

Figure 4 Microphotographs of composites prepared by Method I: (a) unsintered eutectic, (b) sintered eutectic, (c) eutectic + 10 wt % glass, (d) eutectic + 20 wt % glass.

microstructures suggest that nearly spherical glass particulates are uniformly distributed in the host matrix.

To understand the transport mechanism microscopically in the present composites, the relaxation frequency was determined from the peak frequency f_p of the imaginary part of the impedance at various temperatures. Thus, f_p values when plotted as a function of $10^3/T$ (Fig. 7) show an Arrhenius behaviour. According to Salamon [19], the transport of the charge carriers can be visualized as the ions hopping from one site to a nearby vacant site by transversing a barrier of height ΔE (activation energy) at a rate

$$f_p = f_0 \, e^{-\Delta E/kT} \quad (1)$$

called the jump frequency. Here, f_0 is the attempt frequency which is comparable to the phonon frequency and is often taken as a frequency of oscillation of the ion within the cell associated with its lattice site. The activation energies ΔE, calculated using Equation 1, are summarized in Table II along with values obtained from the equation $\sigma = \sigma_0 \, e^{-\Delta E/kT}$ and the conductivities at 553 and 433 K. From this table it can be seen that the activation energies calculated from

TABLE II Comparison of conductivity of $6Li_2SO_4$–$4Li_2CO_3$ eutectic samples prepared by Method I and Method II, along with the activation energies determined from equations $f_p = f_0 \, e^{-\Delta E/kT}$ and $\sigma = \sigma_0 \, e^{-\Delta E/kT}$

	Method I				Method II		
	Host eutectic	+ 10 wt % glass	+ 20 wt % glass	+ 30 wt % glass	Host eutectic	+ 10 wt % glass	+ 20 wt % glass
Conductivity at 553 K (Ω^{-1} cm^{-1})	2.03×10^{-4}	5.7×10^{-4}	9.06×10^{-4}	1.44×10^{-4}	1.8×10^{-4}	2.27×10^{-3}	5.10×10^{-3}
Conductivity at 433 K (Ω^{-1} cm^{-1})	3.26×10^{-7}	3.26×10^{-6}	9.20×10^{-6}	5.17×10^{-6}	6.83×10^{-7}	4.63×10^{-5}	1.13×10^{-4}
Activation energy from $\sigma = \sigma_0 \, e^{-\Delta E/kT}$ (eV)	1.091	0.930	0.880	0.903	1.050	0.684	0.635
Activation energy from $f_p = f_0 \, e^{-\Delta E/kT}$ (eV)	1.092	0.926	0.879	0.910	1.082	0.691	0.6422

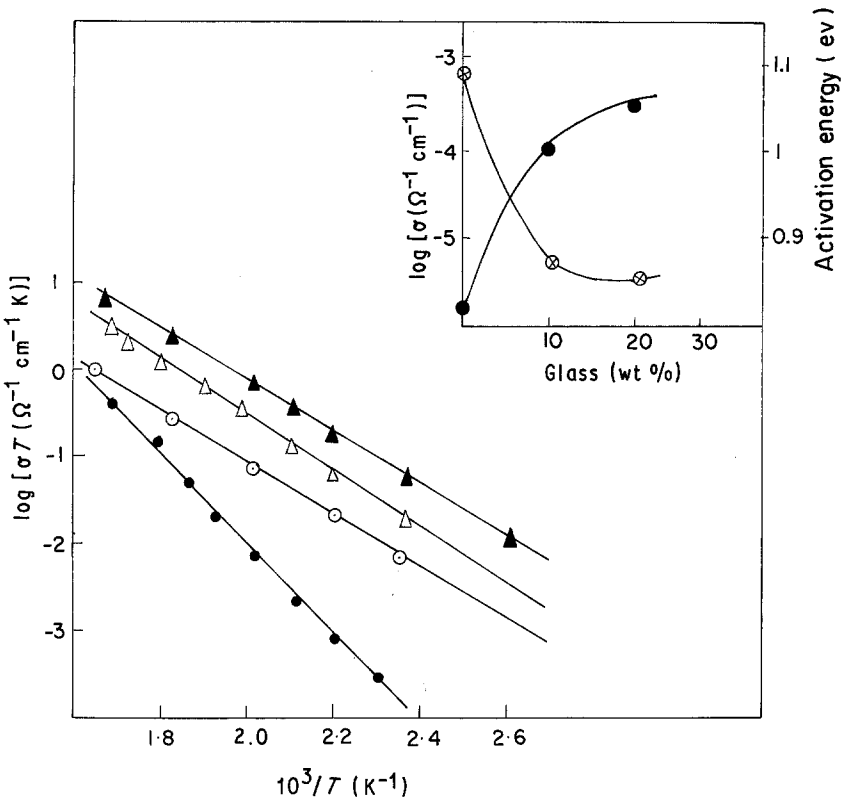

Figure 5 Variation of log σT with $10^3/T$ for samples prepared by Method II: (●) $6Li_2SO_4$–$4Li_2CO_3$ eutectic, (⊙) $7Li_2O$–$3B_2O_3$ glass, (△) eutectic + 10 wt % glass, (▲) eutectic + 20 wt % glass. Inset: (●) log σ and (⊗) activation energy against wt % glass.

both methods are comparable within the experimental error. Sarkar and Nicholson [20] have observed similar results in the case of the CeO_2–Y_2O_3 system. Furthermore, the decrease in the activation energy with increase in concentration of glass dispersoid may be due to an increased number of defects as a result of defect-induced surface interactions at glass–crystalline and crystalline–crystalline interfaces [21]. From Table II it can also be seen that the conductivity enhancement is higher at lower temperatures (< 433 K) compared with that at higher temperatures (> 553 K). These results are in good agreement with the space-charge theory of composites [16].

It is also interesting to note that the samples prepared by Method II show a maximum enhancement in the conductivity, which is about three orders of magnitude at low temperature (< 433 K) in the case of 20 wt % glass-dispersed composite, compared with that of the host system. On the other hand, in the case of samples prepared by Method I the maximum enhancement in the conductivity is about two orders of magnitude at the same temperature. The large enhancement in the conductivity of the composite with 20 wt % glass prepared by Method II compared with Method I may be attributed to the following points.

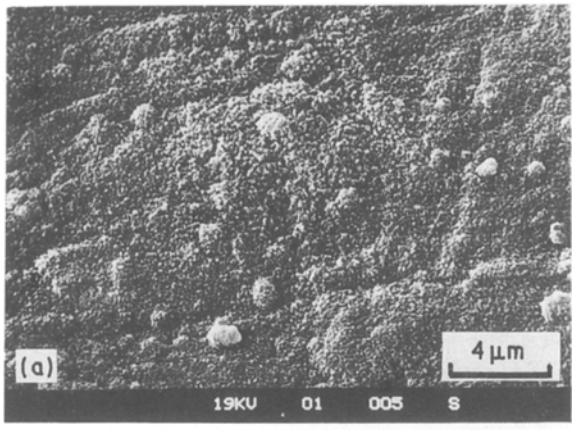

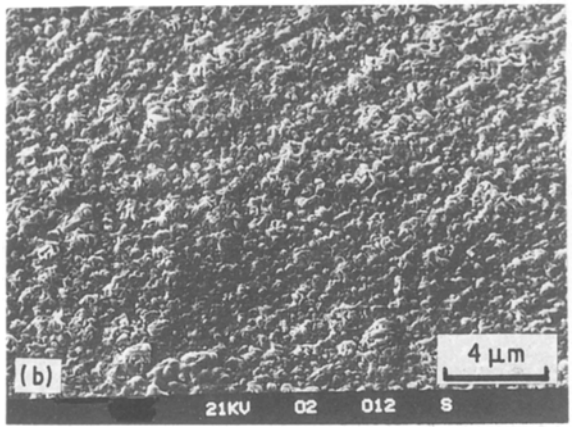

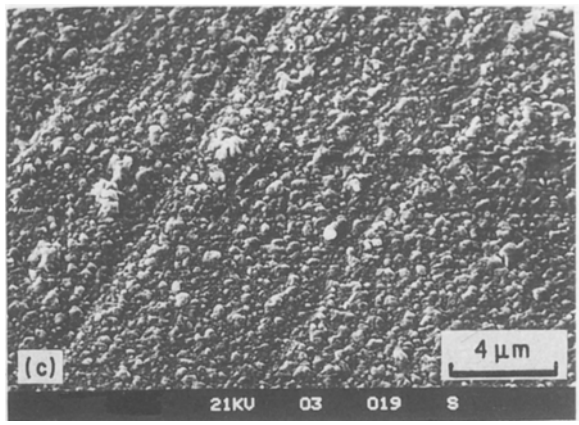

Figure 6 Microphotographs of composites prepared by Method II: (a) host system, (b) eutectic + 10 wt % glass, (c) eutectic + 20 wt % glass.

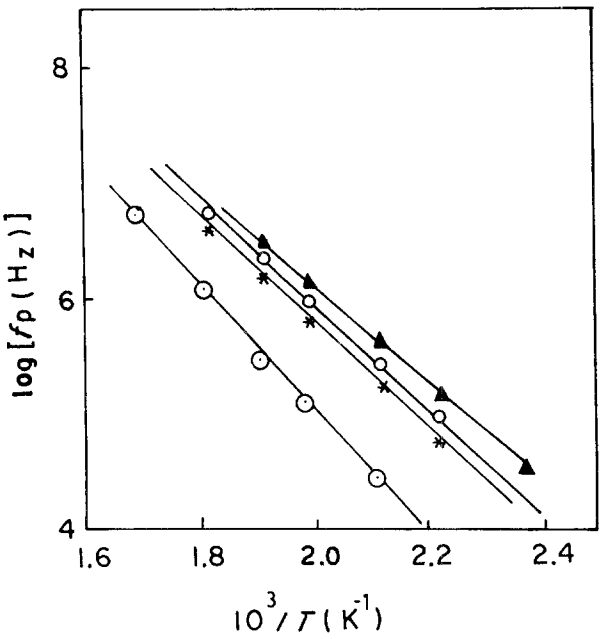

Figure 7 Variation of $\log f_p$ with $10^3/T$ for composites prepared by Method I: (⊙) eutectic, (●) eutectic + 10 wt % glass, (▲) eutectic + 20 wt % glass, (x) eutectic + 30 wt % glass.

(i) In the sample prepared by Method I (sintering) there are voids, unlike the sample prepared by Method II (quenching) (as evidenced by Figs 4d and 6c). These voids hinder the mobility of the charge carriers and consequently reduce the conductivity.

(ii) Due to sintering of the pellet the grains grow in size, whereas no such effect has been observed in the quenched sample.

(iii) The $6Li_2SO_4$–$4Li_2CO_3$ eutectic exhibits a solid–solid phase transition at 723 K. In the case of the quenched sample the transition temperature reduces to 693.5 K, whereas in the case of the sintered sample prepared by Method I it reduces to 686 K (Table III). The lower the transition temperature, the higher is the conductivity.

The enhancement in the ionic conductivity as a result of the dispersion of an ionically conducting glassy phase in the matrix of $6Li_2SO_4$–$4Li_2CO_3$ is an interesting phenomenon, and may be understood in the light of the space-charge model proposed by Jow and Wagner [22]. On the basis of this model, the increased conductivity in composites is attributed to the increased charge carriers forming a space-charge layer near the surface of the dispersoid.

It is worth mentioning that the models developed so far in the area of composites are limited to either conducting–conducting (MX/MX′) or conducting–non-conducting systems (MX/A). The present system is different than these two because of its three ionically conducting constituents, i.e. $7Li_2O$–$3B_2O_3$ glass, β-Li_2SO_4 and Li_2CO_3. The most conducting one is the glassy phase (dispersoid) when compared with Li_2SO_4 and Li_2CO_3. The total conductivity of the glass-dispersed solid electrolyte system may be considered as the contributions from (a) Li_2SO_4 and (b) Li_2CO_3 polycrystalline phases, (c) Li_2O–B_2O_3 glass dispersoid and (d) the interfacial region between these three phases. The observed conductivity is much higher than that of each of the individual phases. Therefore,

TABLE III DTA analysis of 20 wt % glass-dispersed $6Li_2SO_4$–$4Li_2CO_3$ eutectic prepared by Method I and Method II

Sample	Melting point (K)	Glass transition temperature, T_g (K)	Solid-state transition temperature, T_c (K)	ΔT_c* (K)
Li_2SO_4–Li_2CO_3 (eutectic)	843.1	–	823	–
Eutectic + 20 wt % dispersed glass (prepared by Method I)	817	389.8	796.5	26.1
Eutectic + 20 wt % dispersed glass (prepared by Method II)	816	475.3	786.1	36.9

*Decrease in transition temperature (solid state) with reference to pure eutectic.

an enhancement in the total conductivity may be due to (i) increase in the concentration of the charge carriers forming a diffuse space-charge layer [23], and (ii) the enhanced ionic conductivity in or near the crystalline–glass interface due to the formation of more distorted lattice structures. This is strongly supported by the activation energy results discussed earlier. Further, at higher concentrations of dispersoid (> 20 wt %), the voids are formed as a result of the agglomeration of these particulates, which in turn reduces the conductivity.

4. Conclusion

The dispersion of glass in $6Li_2SO_4$–$4Li_2CO_3$ enhances the ionic conductivity by about three orders of magnitude at temperature $\leqslant$ 433 K as compared with the host $6Li_2SO_4$–$4Li_2CO_3$ eutectic. The particle size, voids and distribution of a second insoluble phase in the composite play vital roles in the conduction mechanism. Thus, the dispersion of a glassy phase into a crystalline matrix provides a new approach for ionic conductivity enhancement in solid electrolytes.

Acknowledgements

The authors thank DRDO, New Delhi, for financial support to carry out this work. We would also like to express our gratitude to Dr V. K. Deshpande for his valuable suggestions.

References

1. R. W. POWERS and S. P. MITOFF, in "Solid Electrolytes" edited by P. Hagenmuller and V. VanGool (Academic, New York, 1978) Ch. 9.
2. M. A. K. L. DISSANAYAKE and B. E. MELLANDER, *Solid State Ionics* **21** (1986) 279.
3. V. K. DESHPANDE and K. SINGH, *J. Power Sources* **10** (1983) 191.
4. *Idem*, *Solid State Ionics* **8** (1983) 319.
5. K. SINGH and V. K. DESHPANDE, *ibid.* **7** (1982) 295.
6. K. SINGH, S. S. BHOGA and F. C. RAGHUWANSHI, *Bull. Mater. Soc.* **9** (1987) 263.
7. N. KIMURA and M. GREENBLATT, *Mater. Res. Bull.* **19** (1984) 1653.
8. V. K. DESHPANDE, F. C. RAGHUWANSHI and K. SINGH, *Solid State Ionics* **18/19** (1986) 378.

9. A. R. RODGER, I. KUWANO and A. R. WEST, *ibid.* **15** (1985) 185.
10. K. SINGH and S. ROKADE, *J. Power Sources* **13** (1984) 151.
11. V. K. DESHPANDE and K. SINGH, in "Materials for Solid State Batteries", edited by B. V. R. Chowdhari and S. Radhakrishna (World Scientific, Singapore, 1986) p. 313.
12. V. K. DESHPANDE, S. ROKADE and K. SINGH, in Proceedings of 6th Risø International Symposium on Metallurgy and Materials Science, Denmark, edited by F. W. Poulsen, N. H. Andersen, K. Clausen, S. Skaarup and O. T. Sørensen (GH-Tryk I/s, Odense, Denmark, 1985) p. 227.
13. A. V. CHADWICK, J. H. STRANGE and M. R. WARBOYS, *Solid State Ionics* **9-10** (1983) 91.
14. J. MAIER, in Proceedings of NATO Summer School on Science and Technology of Fast Ion Conductors (1987) p. 215.
15. C. C. LIANG, *J. Electrochem. Soc.* **120** (1973) 1289.
16. F. W. POULSEN, in Proceedings of 6th Risø International Symposium on Metallurgy and Materials Science, Denmark, edited by F. W. Poulsen, N. H. Andersen, K. Clausen, S. Skaarup and O. T. Sørensen (GH-Tryk I/s, Odense, Denmark, 1985) p. 67.
17. V. K. DESHPANDE and K. SINGH, *Solid State Ionics* **6** (1982) 152.
18. C. LIQUAN, in "Materials for Solid State Batteries", edited by B. V. R. Chowdari and S. Radhakrishna (World Scientific, Singapore, 1986) p. 69.
19. M. B. SALAMON, in "Physics of Super Ionic Conductors", edited by M. B. Salamon (Springer, Heidelberg, 1979) p. 2.
20. P. SARKAR and P. S. NICHOLSON, *Solid State Ionics* **21** (1986) 49.
21. J. MAIER, in Proceedings of 6th Risø International Symposium on Metallurgy and Materials Science, Denmark, edited by F. W. Poulsen, N. H. Andersen, K. Clausen, S. Skaarup and O. T. Sørensen (GH-Tryk I/s, Odense, Denmark, 1985) p. 153.
22. T. JOW and J. B. WAGNER Jr, *J. Electrochem. Soc.* **126** (1979) 1963.
23. J. B. PHIPPS and D. H. WHITMORE, *Solid State Ionics* **9/10** (1983) 123.

Received 17 January
and accepted 11 May 1989